ACCSCIENCE PUBLISHING

Journal of Seismic Exploration

ARTICLE

High-precision full-waveform inversion velocity modeling and broadband processing for a deepwater exploration of the South China Sea

Wei Liu[1], Yi Liao[2], Jie Cui[3]*, Ning Zhang[1], Guo Dong Zhang[2], Zi Jing Gong[3], Rong Li[3], Lian Lian Liu[3], and Miaoyang Yuan[3]

[1]China National Offshore Oil Corporation Ltd. Zhanjiang Branch, Zhanjiang, Guangdong, China

[2]China National Offshore Oil Corporation Ltd. Hainan Branch, Haikou, Hainan, China

[3]Department of Digital and Integration, SLB, Beijing, China

(This article belongs to the *Special Issue: Full Waveform Inversion Methods and Applications for Seismic Data in Complex Media*)

Abstract

In deepwater fields, drilling costs are extremely high, and the "one sand, one well" situation is common, in which a single well must control an overly large area of the gas field. Structural accuracy decreases in areas distant from the well locations, making gas reservoir prediction and sand body delineation challenging due to the limited resolution of seismic data. To address these challenges, this study applied high-precision full-waveform inversion (FWI) velocity modeling and broadband imaging technology in a deepwater exploration of the South China Sea. In the preprocessing stage, based on the geological challenges and features of the acquired seismic data, we selected appropriate signal-processing methods and optimized the algorithms and parameter sets, successfully developing a customized broadband processing workflow specifically tailored for deepwater applications. The entire broadband processing sequence effectively supported subsequent FWI modeling. During the imaging stage, FWI was successfully applied for the 1st time in the deepwater of the South China Sea. Together with Q pre-stack depth migration, this integrated approach effectively addressed challenges in structural depth prediction and significantly improved imaging resolution. This study provided real-time support for gas field development and optimized the well placement for deepwater development.

Keywords: Deepwater; Low-frequency noise attenuation; Broadband processing; Full-waveform inversion

***Corresponding author:**
Jie Cui
(jcui2@slb.com)

Citation: Liu W, Liao Y, Cui J, *et al*. High-precision full-waveform inversion velocity modeling and broadband processing for a deepwater exploration of the South China Sea. *J Seismic Explor*. 2026;35(1):139-150.
doi: 10.36922/JSE025410084

Received: October 11, 2025

Revised: December 9, 2025

Accepted: December 15, 2025

Published online: January 7, 2026

1. Introduction

Since the mid-1980s, there has been an increase in exploration activities and challenges related to new discoveries in onshore and shallow-water oil and gas fields, along with the evolution of exploration and development technologies. Due to this advancement, deepwater oil and gas exploration and development have attracted increasing attention and expanded significantly over the past decade. Deepwater exploration has become a strategic focus in global hydrocarbon exploration.[1,2]

With the increasing depth of exploration targets in deepwater fields, traditional seismic data processing and interpretation techniques often fail to meet the requirements of deepwater oil and gas exploration. Several new techniques and methods[3] have been specifically developed for deepwater exploration, among which seismic velocity modeling remains a critical stage.

The Lingshui gas field is the first deepwater gas field in China discovered through independent exploration. Due to the extremely high drilling costs in deepwater, exploration wells are sparsely distributed, resulting in excessively large control ranges for individual wells, and significantly reducing the structural accuracy for areas far away from well locations. In the field, the well control is limited, and the accuracy of single sand body delineation cannot meet the exploration and production requirements. Moreover, due to the limited resolution of seismic data, it is challenging to identify and predict the distribution of shale interlayers within the gas field. In this study, we applied high-precision full-waveform inversion (FWI) technology to explore the Lingshui gas field.

To address the challenges of deepwater exploration, we developed a signal processing workflow including low-frequency noise attenuation and low-frequency signal expansion. We evaluated multiple combinations of noise-attenuation algorithms to improve the signal-to-noise ratio. The anomalous amplitude attenuation (AAA) and curvelet transform are applied to suppress low-frequency noise while preserving low-frequency signals.[4,5] Combined with adaptive deghosting technology, the low-frequency signal is effectively enhanced.[6]

The entire workflow provided the input data required for subsequent high-precision FWI velocity modeling. FWI is a high-precision, high-resolution methodology for inverting subsurface properties defined by the wave equation. It reconstructs the earth model using amplitude and phase information from seismic data. Since Lailly and Tarantola introduced the concept of FWI to seismic exploration,[7,8] this technique has received increasing attention and has been widely studied and applied in seismic velocity modeling.

Conventional FWI minimizes the least-squares difference between the acquired and the predicted data. It is exposed to cycle-skipped solutions that cause the process to converge to local minima rather than the global minima. In this study, a robust adaptive FWI based on a phase shift objective function is first applied to construct the velocity model, correcting erroneous background models, mitigating cycle-skipping issues, and improving the robustness of FWI when using inaccurate initial models.[9,10]

Based on the challenges of deepwater exploration, the FWI velocity model building was implemented in three bands. In Band 1 and Band 2, data after noise attenuation were used as input to FWI. To introduce more information for velocity updates in deep layers, data after deghosting and multiple attenuation were used as the input data in the Band 3 FWI. The Band 1 applied an adaptive FWI based on a phase-only objective function, while the latter two bands used the conventional least-squares FWI whose objective function was constructed using amplitude residuals between observed and synthetic data. This study also conducted sophisticated quality control (QC) in each FWI band, including interleave shot gather QC, well-log velocity QC, and mistie analysis QC. By applying FWI to derive a high-accuracy subsurface velocity model, we effectively provided real-time support for the oilfield development plan for the first self-owned deepwater giant gas field in China, guided the optimization of well placement, and saved a significant amount of cost for drilling operations.

2. Methods

2.1. Amplitude-preserved low-frequency noise attenuation

The success of an FWI relies on certain requirements for the input data. Seismic data acquired in deepwater areas always suffer from strong low-frequency noise, such as swell noise. To enhance the signal-to-noise ratio of seismic data, a customized noise suppression workflow was designed using a combination of methods across multiple domains, algorithms, and frequency bands.

Specifically, we applied a combination of the AAA and curvelet transform for low-frequency noise attenuation. AAA is a method that suppresses random noise by transforming seismic data into the frequency domain within a certain time window. It utilizes a spatial median filter to compare the amplitude of the seismic trace with the average amplitude of adjacent traces, determining whether it is a noisy trace. Once a trace is identified as noise, it is either attenuated by multiplying it by a coefficient or replaced by the interpolation of neighboring seismic traces. This method has been used to suppress low-frequency noise in low-pass frequency bands.

For residual low-frequency swell noise, we innovatively used a residual coherent noise suppression method in the curvelet domain. Similar to the Fourier transform, which decomposes different frequency components into sine and cosine functions and reconstructs them in the time-x domain, curvelet transforms employ a more precise and sophisticated transformation that prevents signal loss due to time-frequency domain conversion. Figure 1 shows the original shot gather, post-noise suppression shot gather, and the suppressed noise. The results clearly demonstrate that swell noise is effectively suppressed. Overall, the study

employed a combination of AAA and curvelet transform techniques for effective noise suppression in deepwater seismic data, which is essential for accurate FWI velocity modeling and provides a solid foundation for subsequent imaging.

2.2. Adaptive deghosting

When acquiring marine seismic data, to reduce the influence of sea surface swell noise, streamers are typically placed at a certain depth to record seismic data. As an interface between air and seawater, the sea surface is a strong reflector for seismic waves. When the upgoing reflected seismic wave reaches the sea surface, it reflects back to the water bottom with reversed polarity and is recorded by the hydrophone. This downward reflection wave is referred to as a ghost reflection or ghost wave. Both the seismic reflection wave and the ghost wave are recorded by the streamer and interfere with each other, causing notch phenomena in the spectrum. The waveform of the reflection signal is also changed by the ghost waves; the amplitude at corresponding notch frequencies is significantly reduced, affecting the resolution of seismic data. Therefore, adaptive deghosting technology is an effective method for suppressing ghost waves, eliminating the notch effects caused by these waves, and restoring the low-frequency components in the seismic signal. The expansion of low-frequency components is crucial for FWI.

Over the past few decades, various methods have been developed for ghost wave suppression, such as the inverse scattering series method[11] and the frequency-wavenumber domain wavefield extrapolation method.[12] However, due to various constraints during the in-field seismic data acquisition, ghost suppression methods do not always yield satisfactory results. In this study, we applied a ghost wave suppression method proposed by Rickett *et al.*[6] The algorithm adaptively solves the upgoing wavefield and ghost wave delays in the local plane-wave domain (Tau-p domain). The seismic data, denoted as d in **Equation 1**, is sparsely decomposed by minimizing the objective function shown in **Equation 1**:

$$\chi(x,\Delta t)=\left\|W\left[SG\left(\Delta t\right)x-d\right]_2^2+\left\|x_1\right\|\right\| \quad (1)$$

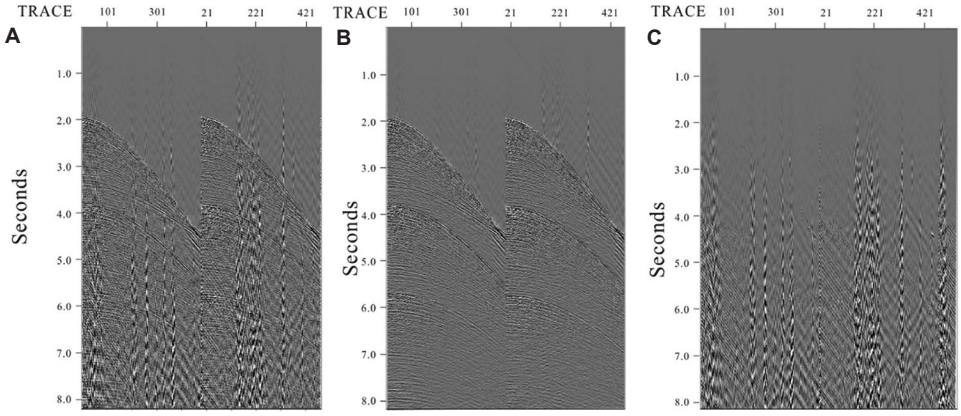

Figure 1. Comparison before and after noise suppression (A) Original shot gathers. (B) Post-noise suppression shot gather. (C) Suppressed noise.

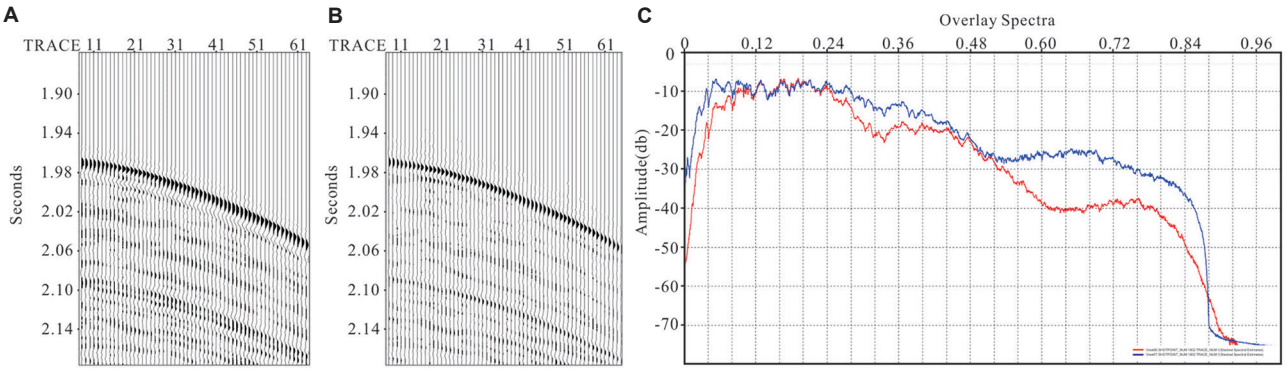

Figure 2. QC of the result before and after deghosting. (A) Shot gather before adaptive deghosting, (B) shot gather after adaptive deghosting, and (C) spectral analysis of the near-offset gather before (red) and after (blue) adaptive deghosting.

Where x represents the coefficients of the plane-wave basis, Δt is the delay time, W represents a weighting function that can be used to balance the amplitude of the input seismic data, S is the plane-wave synthesis factor, and $G(\Delta t)$ represents the ghost wave suppression factor. The adaptive deghost method utilizes receiver depth information to suppress ghost waves in the shot gather. **Equation 1** defines the objective function used in the inversion and quantifies the misfit between the observed and modeled data. Physically, this equation quantifies how well the simulated wavefield reproduces the recorded wavefield. The first term typically involves the squared L2 norm of the data residuals, ensuring that the inversion minimizes amplitude and phase differences between observed and modeled traces. The algorithm is robust even when the data contains strong noise. In addition, it can suppress ghost waves, correct phase information, mitigate notch effects, enhance low-frequency energy, broaden the frequency spectrum, and restore a more accurate wavelet. Particularly, the expansion of low-frequency information is crucial for the FWI used in this study. In this paper, the adaptive deghosting was only applied to streamer ghosts. Figure 2A and B show the shot gather before and after adaptive deghosting; the comparison shows that the ghost wave was effectively suppressed. The spectral analysis of the near-offset gather before and after adaptive deghosting is shown in Figure 2C, where the notch in the spectrum is effectively compensated, particularly in the low-frequency signal extension. This results in a solid foundation for subsequent FWI imaging.

2.3. High-resolution FWI velocity model building and imaging

2.3.1. FWI

FWI was applied in this study. It is the most advanced method for building velocity models. FWI is based on the two-way wave equation theory, which is suitable for various data acquisition techniques. It utilizes the full-waveform information to iteratively update the subsurface velocity model.

Compared to conventional tomographic imaging methods, FWI can build a high-precision velocity model that more accurately matches the geological structures. By iteratively minimizing the misfit between observed and modeled waveforms, FWI can accurately capture velocity details. Moreover, FWI benefits from the use of accurately modeled seismic wavelets that closely match the observed data. In addition, low-frequency and long-offset data contribute to the successful convergence of FWI, providing valuable information for resolving complex subsurface structures.

In summary, FWI is a cutting-edge technology for velocity modeling, enabling the estimation of detailed subsurface velocity structure and enhancing our understanding of geological structures.

2.3.2. FWI theory

FWI has gained widespread application in industry over the past few years. Three-dimensional pre-stack acoustic FWI utilizes the two-way wave equation to establish high-

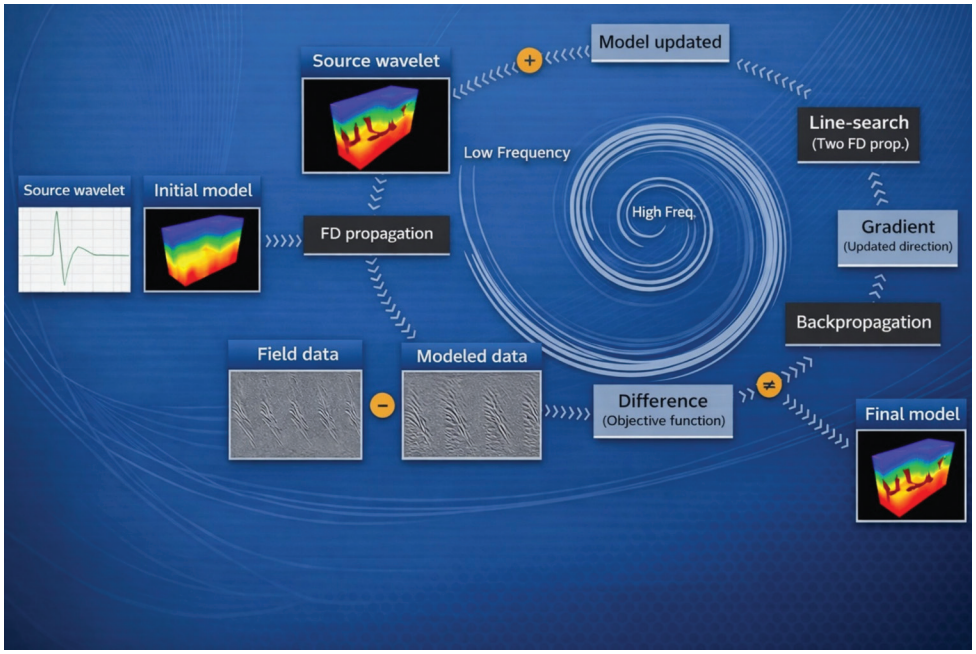

Figure 3. Full-waveform inversion schematic diagram

resolution velocity models. The basic principle of FWI can be summarized as follows:

- Forward modeling: The process begins with forward modeling using an initial velocity model. A synthetic waveform is generated by solving the wave equation, simulating the response of the wavelet to an estimated velocity distribution.
- Misfit calculation: The acquired seismic data is subtracted from the forward-modeled data. This residual represents the misfit between the observed and modeled data, and it forms the objective function of FWI.
- Gradient computation: By applying an algorithm similar to reverse time migration, the gradient is calculated based on the residual waveforms, reflecting the direction of velocity update. The gradient provides information on how to update the velocity model to reduce the misfit.
- Model update: Using gradient information, the velocity model is updated accordingly. The updated model is obtained by minimizing the misfit between the observed and modeled data.
- Iterative process: The forward modeling, misfit calculation, gradient computation, and model update steps are repeated iteratively until convergence is achieved, or until a specified stopping criterion is met.

Figure 3 illustrates the schematic diagram of the theory behind FWI. This process aims to iteratively refine the velocity model, ultimately resulting in a high-resolution velocity model that more accurately matches the observed seismic data.

2.3.3. Adaptive FWI

The FWI method described above is based on conventional least-squares theory. The main limitation of this approach is that it requires a relatively accurate initial velocity model, or that the observed data contain sufficiently rich low-frequency information and long offsets. The traditional FWI algorithm minimizes the difference between the acquired data and the predicted (forward-modeled) data in the least-squares sense. However, there is a risk of encountering cycle-skipping issues, and the objective function can easily get trapped in local minima rather than the global minimum. The objective function is shown in **Equation 2**, where J represents the misfit function, m represents the model, d_0 represents the acquired data, and F[m] denotes the forward operator that simulates the predicted data.

$$\min_{m\in M} J := \frac{1}{2}\sum_{s=1}^{N_s}\left\|F[m](x_r,t)-d_0(x_r,t;s)\right\|^2 \quad (2)$$

In early FWI studies, inversion was typically applied after several rounds of tomography to obtain a more accurate initial model and compensate for missing low-frequency content. Adaptive FWI introduces a robust objective function based on time delays or phase differences between observed and modeled data, thereby reducing cycle skipping and improving tolerance to initial model errors.[9,10] For a single frequency, the travel-time difference (ΔT) between two signals is proportional to the phase difference ($\Delta\varphi$), as shown in **Equation 3**. This allows the inversion to use a phase-only objective function by backpropagating local travel-time differences into model updates. Identifying travel-time differences in the time domain is generally more reliable than estimating phase differences. These local differences can be converted into instantaneous phase errors, representing misaligned phases, and used to compute gradients for velocity updates. Consequently, adaptive FWI can begin with a relatively higher frequency band, improving signal-to-noise ratio and inversion stability.

$$\min_{m\in M} J := \frac{1}{2}\sum_{s=1}^{N_s}\left\|\Delta T\right\|^2 = \frac{1}{2}\sum_{s=1}^{N_s}\left\|\Delta T(\Delta\varphi)\right\|^2 \quad (3)$$

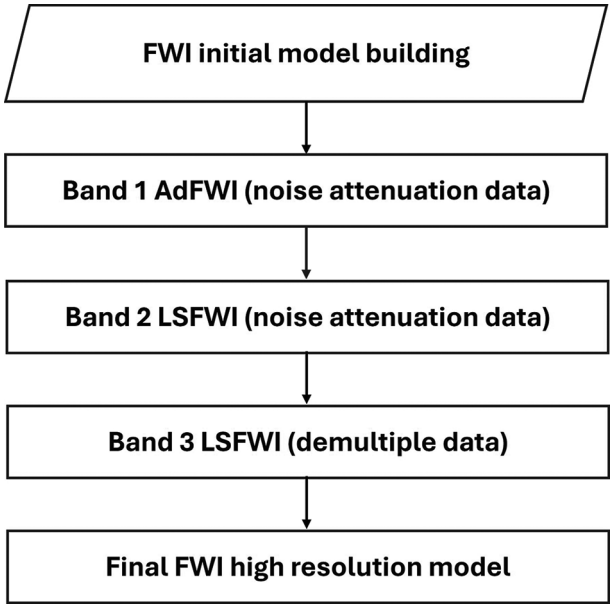

Figure 4. Full-waveform inversion (FWI) velocity model building workflow
Abbreviations: Ad: Adaptive; LS: Least-squares.

2.3.4. FWI velocity model building workflow

For this study, the feasibility of FWI can be summarized as follows:

- Adequate low-frequency signal: The preprocessing stage included fine noise attenuation, which ensured that the low-frequency signal was properly preserved. This is beneficial for the convergence of FWI, as the presence of sufficiently low-frequency signals improves the convergence and stability of the FWI process.

- Sufficient cable length: The target layer depth is around 3,000 m, and the maximum offset is 6,200 m. These allow FWI to reliably estimate the velocity model with high resolution at the target layer depth. The long offset allows for capturing a wide range of reflection angles, enabling better constraints on the velocity model.
- Hybrid velocity update solution: In low-frequency bands, pure data-driven FWI effectively resolves the background velocity. In higher frequency bands, the inversion is integrated with well constraints, incorporating additional information from well logs or borehole data. This hybrid approach enhances the velocity resolution and accuracy, with well data providing valuable guidance to the inversion process.

In summary, the feasibility of FWI in the study is supported by the presence of abundant low-frequency

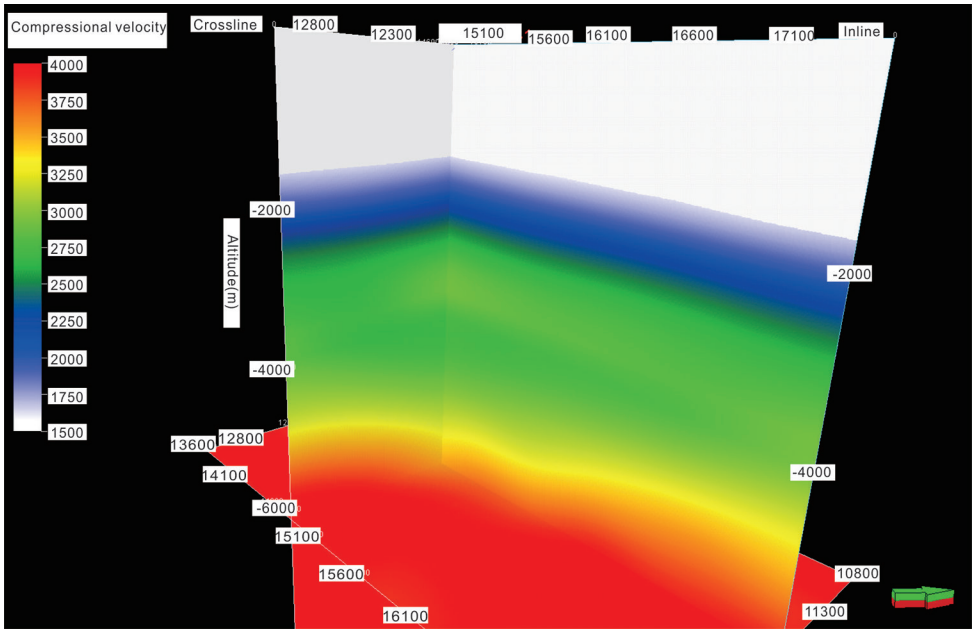

Figure 5. Initial velocity model

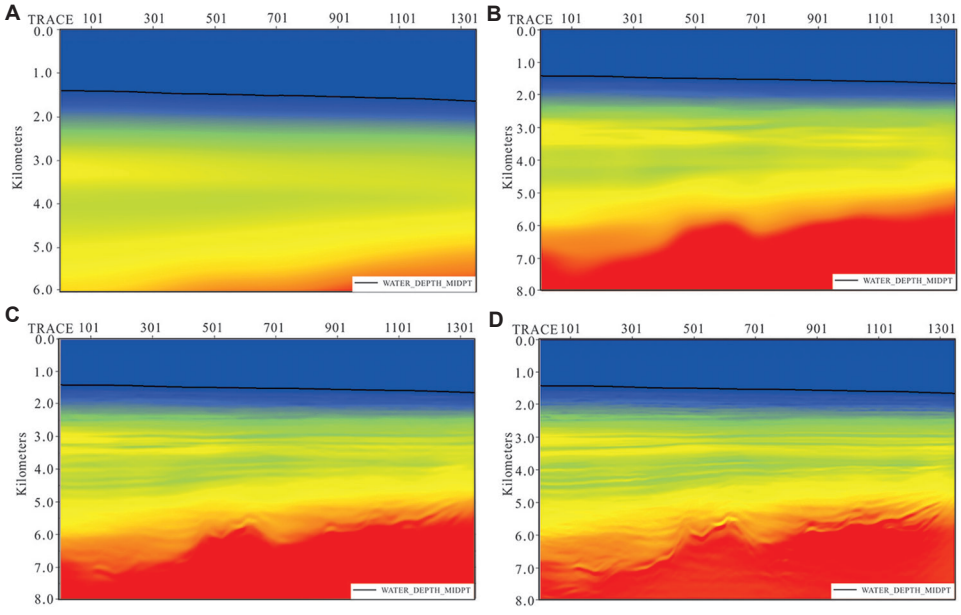

Figure 6. Comparison among different velocity models. (A) Initial velocity model. (B) Adaptive full-waveform inversion (FWI) Band 1 updated velocity model. (C) Least-squares FWI Band 2 updated velocity model. (D) Least-squares FWI Band 3 well-constrained updated final velocity model.

signals, a suitable target layer depth and offset distance, and the utilization of a hybrid FWI approach combining waveform information and well constraints. These factors provide a solid foundation for FWI to achieve a high-resolution and accurate velocity model building.

The detailed FWI modeling workflow is shown in Figure 4. Since the ghost wave interferes with the amplitude and phase of the recorded seismic signals, it is common practice to suppress the ghost waves before applying FWI. A zero-phase wavelet is generated during the finite-difference wavefield simulation without a ghost effect. However, this method relies on high-quality ghost wave suppression, as inadequate ghost suppression will negatively impact FWI. Sun *et al.*[13] demonstrated the successful application of FWI by simulating ghost wave effects in towed-streamer data. Therefore, in this study, the second approach was adopted for FWI in Bands 1 and 2, where only basic noise attenuation was applied to the seismic data for FWI input, with direct arrivals, ghost waves, and multiples included in the inversion. As the velocity model was iteratively updated to incorporate more data for deeper-layer inversion, the input in FWI Band 3 was replaced with full-record-length shot gathers after deghosting and multiple attenuation. The Band 1 update utilized adaptive FWI with a phase-based objective function, while the subsequent two bands' updates employed a traditional least-squares objective function. In the last highest frequency band, well velocities were introduced into FWI as constraints.

3. Results and discussion

In this study, the process of initial model building is as follows. Firstly, the water column velocity was determined based on time–space dip records and was further refined through precise picking. Then, the time-domain velocity model was converted to a depth-domain interval velocity

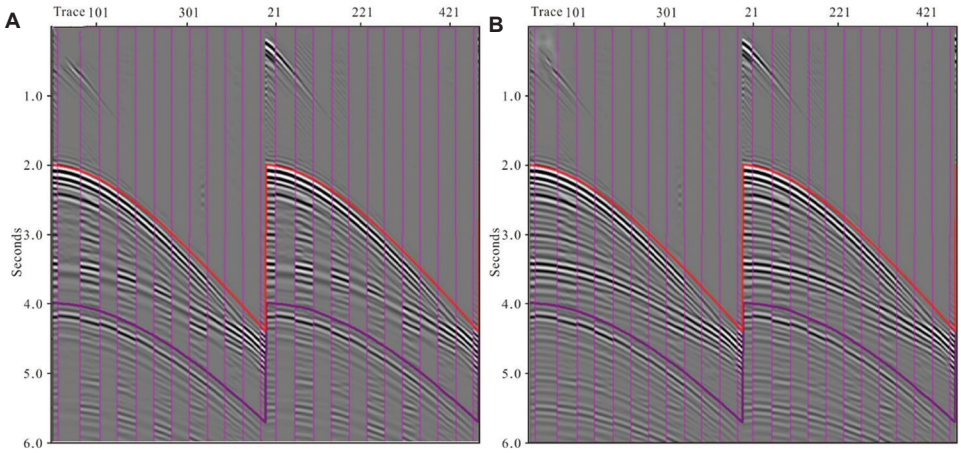

Figure 7. QC of FWI Band 2. (A) Interleaved display before full-waveform inversion (FWI) Band 2. (B) Interleaved display after FWI Band 2.

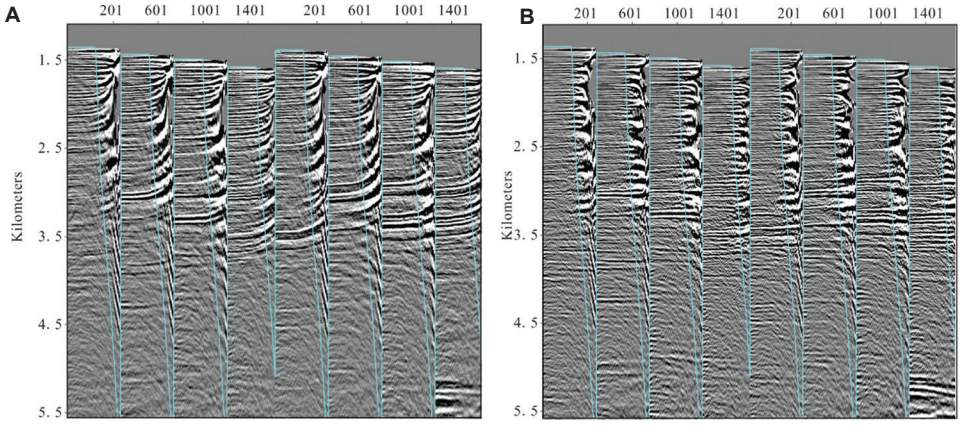

Figure 8. QC of CIP gathers with different velocity models. (A) Common image point (CIP) gathers with the initial model. (B) CIP gathers with the final FWI high-resolution model.

using the Dix formula, followed by the application of large-scale smoothing to the converted velocity model. Finally, incorporating the low-frequency trend of well-log velocity in the target layer enabled the construction of an accurate background velocity at the target zone. The initial velocity model is shown in Figure 5.

A cross-well velocity profile was used as an example to illustrate the FWI modeling process. The initial velocity model is shown in Figure 6A, and the updated velocity model using adjustive FWI with data after noise attenuation is shown in Figure 6B. It can be observed that the updated velocity model captured more details compared to the initial model.

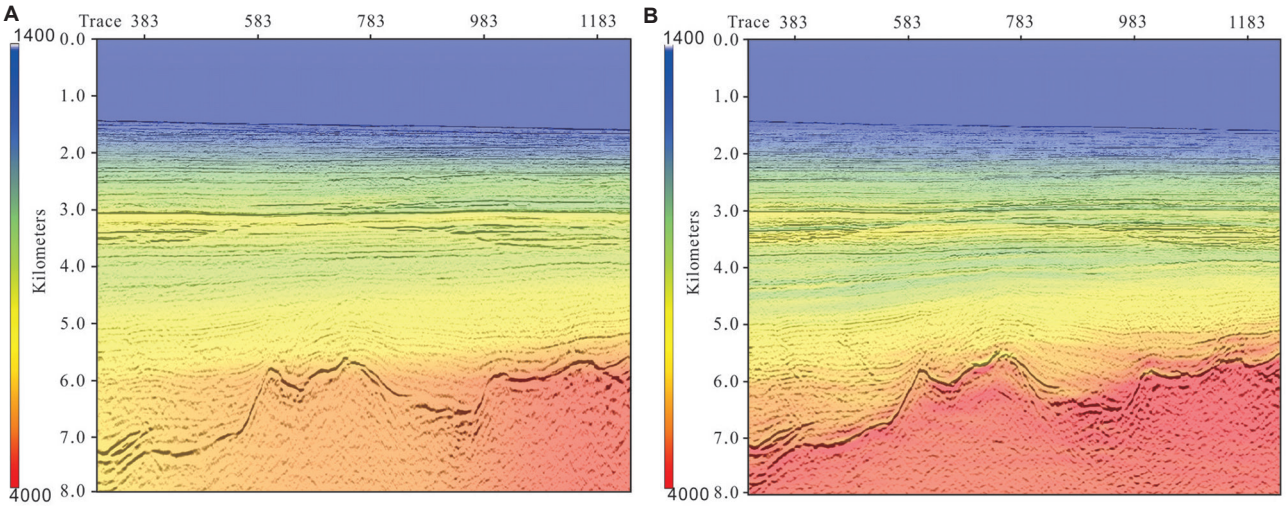

Figure 9. QC of pre-stack depth migration (PSDM) results with different velocity models. (A) Initial velocity model and its Kirchhoff PSDM image overlay. (B) Final full-waveform inversion velocity model and its Kirchhoff PSDM image overlay.

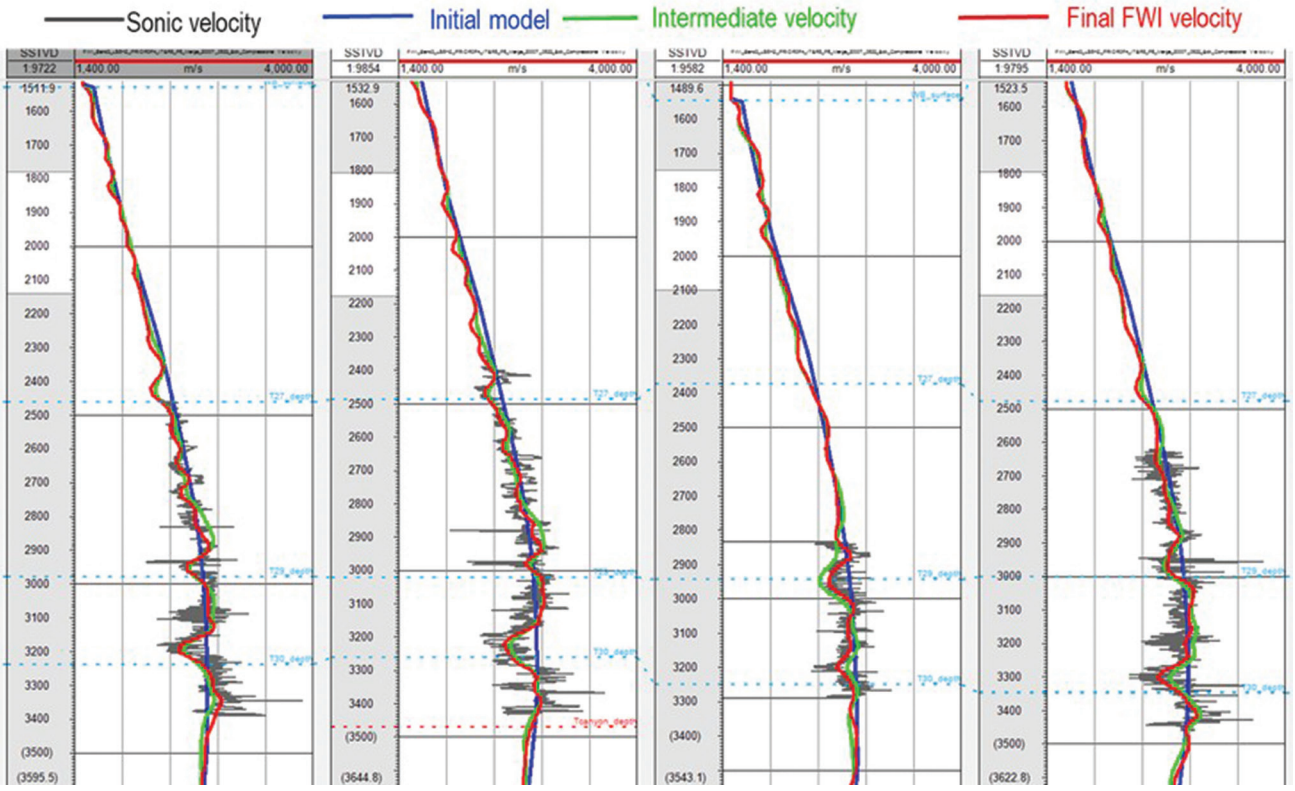

Figure 10. Sonic logging velocity and full-waveform inversion (FWI)-derived velocity comparison

Figure 6C shows the velocity model after the Band 2 least-square FWI update. To incorporate more information for deeper updates, the input data for FWI Band 3 were replaced with full-record-length shot gathers after deghosting and multiple attenuation. The FWI Band 3 employed the least-squares FWI on full record length data and introduced well velocities as constraints. Figure 6D displays the final velocity model after the Band 3 well-constrained FWI. It is clearly shown that deep layers of the velocity model have been updated with abundant details.

During each band of FWI, several iterations were performed for the inversion. It is essential to monitor the convergence of the objective function and the magnitude of the velocity updates. This helps in making optimized decisions regarding the total number of iterations and the frequency of the incremental strategy of FWI updates. Between each FWI band, various QC measures were conducted, including comparing the observed and synthetic shots using an interleave display and verifying the velocity field updates. These QC steps provide a comprehensive assessment of the FWI progress.

Comparisons of observed shots and synthetic shots were used to evaluate the improvement in data matching before and after FWI updates, particularly for the interleaving QC, where the observed and synthetic traces are interleaved and displayed in the same shot gather. In this study, we focused on identifying whether there is any improvement from mismatched patterns to more coherent patterns.

Figure 7 shows the interleaved display comparison before and after the FWI Band 2. The red and purple curves represent the time window used in FWI. It can be observed that after the FWI update, the reflection events in shot gathers became more continuous and smoother, with improved alignment within the time window.

Another QC metric is the assessment of gather flatness. Common image point gathers were selected every 10 km. Gathers from the initial velocity model are shown in Figure 8A, while gathers from the final high-precision FWI model are shown in Figure 8B. It can be observed that the final velocity model yielded a flatter gather set, indicating the effectiveness of the FWI velocity update.

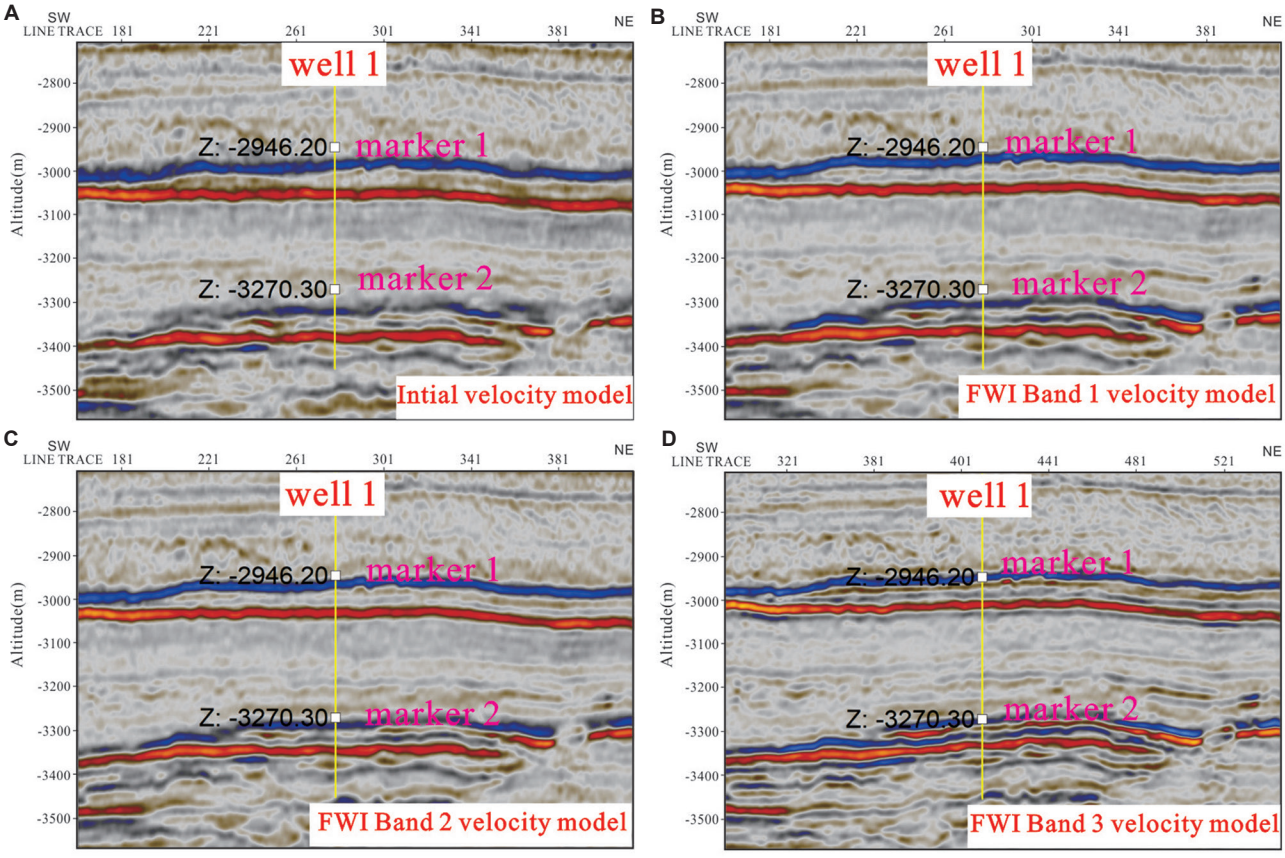

Figure 11. (A-D) Mistie analysis during the velocity update process
Abbreviation: FWI: Full-waveform inversion.

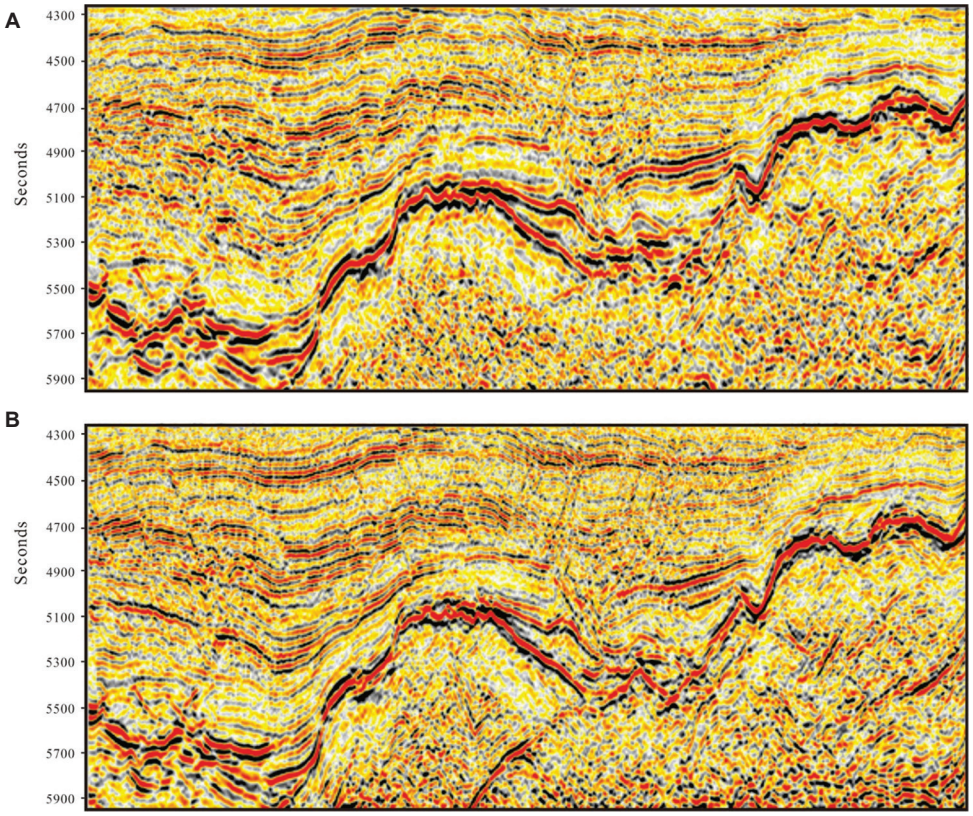

Figure 12. Kirchhoff pre-stack depth migration (PSDM) of the deep zone. (A) Legacy Kirchhoff PSDM image. (B) New reprocessed Kirchhoff PSDM image.

Velocity field QC is also crucial for monitoring the overall trend of the velocity model update during FWI. Figure 9A displays the initial velocity model overlaid with the initial stacking section, while Figure 9B shows the final FWI model overlaid with the final stacking section. The velocity model became more refined with abundant details, and the velocity structure showed better consistency with the subsurface image.

Figure 10 shows the comparisons between well velocity curves and seismic velocity at a specific well location. The black curve represents the sonic velocity, the blue curve represents the low-frequency initial velocity, the green curve represents the intermediate iterated velocity, and the red curve represents the final FWI velocity. It can be observed that the overall trends between the well velocity and updated seismic velocity are relatively well-matched, indicating that FWI has effectively captured the velocity variations and improved the model's accuracy.

Throughout the entire model-building process, mistie analysis was conducted for key FWI iterations. Figure 11 shows the variation of mistie at two key layers from the initial model to the final FWI model. From the figure, it can be observed that the overall mistie converges gradually during the velocity update process.

Figure 12A and B show the Kirchhoff pre-stack depth migration (PSDM) stack profile from the legacy data and the new processed data for the deep zone, respectively. From the comparison, it can be observed that the new processed results exhibited higher resolution, enhanced event continuity, and better imaging of deep-seated faults. Figure 13A and B show the Kirchhoff PSDM comparison for the target zone. For legacy data, in this area, the tectonic contact relationship of different channels was very complex, and it was difficult to distinguish lithology within the channels. From the new reprocessed results, the channel boundary was more focused and sharper in the new data. The channel boundaries were clearly identifiable, showing significant improvement over the legacy data. The enhanced resolution of the new data was particularly helpful for delineating thin sand layers and provided a more accurate channel image. The new results showed significant improvements over the legacy data.

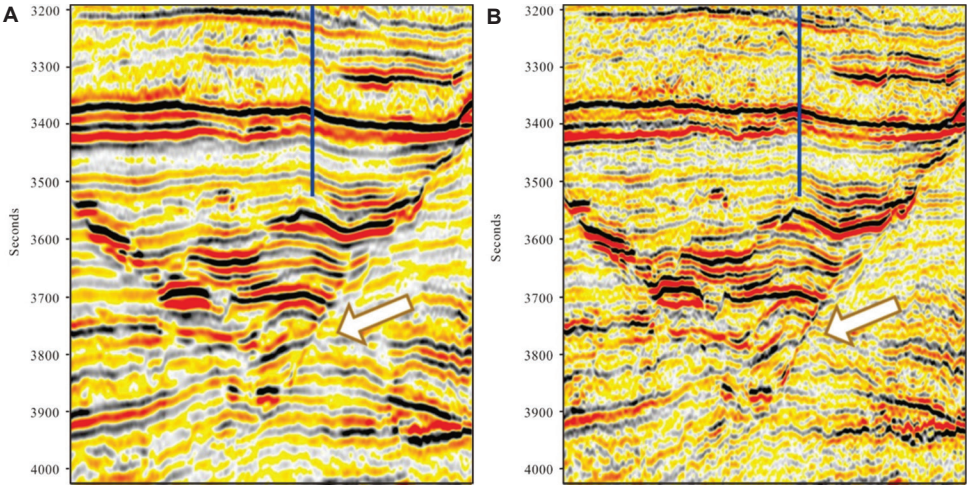

Figure 13. Kirchhoff pre-stack depth migration (PSDM) of the target zone. (A) Legacy Kirchhoff PSDM image. (B) New reprocessed Kirchhoff PSDM image.

4. Conclusion

In this study, we developed a workflow for deepwater seismic data that suppresses low-frequency noise (high signal-to-noise ratio data was obtained through a combination of noise attenuation methods) and expands low-frequency signals (adaptive deghosting) based on the features of the seismic data acquired during a deepwater environment survey in the South China Sea. A subsequent high-precision FWI velocity modeling and imaging technology was applied. This study illustrates the principles, implementation process, and results of FWI, demonstrating significant improvements in processing results. The results show that the signal-to-noise ratio was enhanced, and the bandwidth was expanded, resulting in a high-precision velocity model and high-quality imaging results.

The combination of the AAA and curvelet transform was introduced as an innovative approach. Low-frequency noise was successfully suppressed using this workflow; at the same time, the resulting high signal-to-noise ratio low-frequency data provided a solid foundation for FWI velocity imaging.

The adaptive deghosting technology was applied, which suppressed receiver ghost waves and compensated for the notch effect in the frequency spectrum. More importantly, it enhanced the signal in the low-frequency end, which is crucial for subsequent FWI inversion.

In the early stage of FWI inversion, a robust adaptive FWI was used to reduce the risk of cycle skipping. Then, least-squares FWI was applied using full-record-length shot gathers after multiple attenuation as input data to further update the velocity distribution of the deeper layers. Well velocity was also introduced for well-constrained least-squares FWI. Finally, a high-precision velocity model and high-quality imaging results were derived.

This processing workflow yielded satisfactory results in seismic data processing within the study area, establishing a fit-for-purpose processing workflow for deepwater exploration. The integrated solution provided a data foundation for subsequent FWI velocity modeling. By combining PSDM with FWI, the technique was successfully applied in a deepwater area of the South China Sea, resolving the challenges of depth prediction and enhancing imaging resolution. This project effectively provided real-time support for gas-field development and well-trajectory optimization. Finally, a high-precision velocity model and high-quality imaging results were obtained, providing a data foundation for subsequent property inversion and interpretation work. The processing workflow in this study can be extended to seismic data acquired in similar marine environments.

Acknowledgments

None.

Funding

None.

Conflict of interest

The authors declare that they have no competing interests.

Author contributions

Conceptualization: Wei Liu, Jie Cui, Yi Liao
Formal analysis: Ning Zhang
Investigation: Guo Dong Zhang
Methodology: Rong Li, Lian Lian Liu
Visualization: Zi Jing Gong, Jie Cui, Miaoyang Yuan

Writing–original draft: Wei Liu, Jie Cui, Zi Jing Gong
Writing–review & editing: Yi Liao, Ning Zhang, Guo Dong Zhang, Rong Li, Lian Lian Liu, Miaoyang Yuan

Availability of data

Data will be made available on request to the corresponding author. All data analyzed have been presented in the paper.

References

1. Khain VE, Polyakova ID. Oil and gas potential of deep- and ultradeep-water zones of continental margins. *Lithol Miner Resour*. 2004;39(6):530-540.

   doi: 10.1023/b: limi.0000046956.08736.e4

2. Pettingill HS, Weimer P. Worlwide deepwater exploration and production: Past, present, and future. *Lead Edge*. 2002;21(4):371-376.

   doi: 10.1190/1.1471600

3. Wang W. Difficulties and development trend of exploration in deep and ultra deep water area. *China Pet Explor*. 2010;15(4):71-75. [Article in Chinese].

4. Candès E, Demanet L, Donoho D, Ying L. Fast discrete curvelet transforms. *Multiscale Model Simul*. 2006;5(3):861-899.

   doi: 10.1137/05064182x

5. Naghizadeh M, Sacchi MD. Beyond alias hierarchical scale curvelet interpolation of regularly and irregularly sampled seismic data. *Geophysics*. 2010;75(6):WB189-WB202.

   doi: 10.1190/1.3509468

6. Rickett JE, Van Manen DJ, Loganathan P, Seymour NY. Slanted-Streamer Data-Adaptive Deghosting with Local Plane Waves. In: *Presented at: 76th EAGE Conference and Exhibition*; 2014.

   doi: 10.3997/2214 4609.20141453

7. Lailly P. The Seismic Inverse Problem as a Sequence of Before Stack Migrations. In: Bednar JB, Robinson E, Weglein AR, editors. *Conference on Inverse Scattering-Theory and Application*. SIAM; 1983. p. 206-220.

8. Tarantola A. Inversion of seismic reflection data in the acoustic approximation. *Geophysics*. 1984;49(8):1259-1266.

   doi: 10.1190/1.1441754

9. Jiao K, Sun D, Cheng X, Vigh D. Adjustive Full Waveform Inversion. Proceedings of the *SEG Technical Program Expanded Abstracts* 2015; 2015. pp. 1091-1095.

   doi: 10.1190/segam2015-5901541.1

10. Vigh D, Jiao K, Cheng X, Sun D, Kapoor J, Lewis O. Efficiently using full-waveform inversion in the velocity model building flow. In: *Presented at: 78th EAGE Conference and Exhibition*; 2016.

    doi: 10.3997/2214-4609.201601191

11. Wang FF, Li JY, Chen XH. Deghosting method based on inverse scattering series. *Chin J Geophys*. 2013; 56(5):1628-1636. [Article in Chinese].

    doi: 10.6038/cjg20130520

12. Fokkema JT, Van Den Berg PM. *Seismic Applications of Acoustic Reciprocity*. Amsterdam: Elsevier; 1993.

13. Sun D, Jiao K, Cheng X, Vigh D. Compensating for source and receiver ghost effects in full waveform inversion and reverse time migration for marine streamer data. *Geophys J Int*. 2015;201:1507-1521.

    doi: 10.1093/gji/ggv089